Large Strain Stress Relaxation and Recovery Behavior of Amorphous Ethylene–Styrene Interpolymers

ARTICLE *in* MACROMOLECULES · OCTOBER 1999

Impact Factor: 5.8 · DOI: 10.1021/ma990938g

Large Strain Stress Relaxation and Recovery Behavior of Amorphous Ethylene−Styrene Interpolymers

H. Y. Chen,[†] E. V. Stepanov,[†] S. P. Chum,[‡] A. Hiltner,*[,†] and E. Baer[†]

Department of Macromolecular Science and Center for Applied Polymer Research (CAPRI), Case Western Reserve University, Cleveland, Ohio, 44106-7202, and Polyethylene and INSITE Technology R & D, The Dow Chemical Company, Freeport, Texas, 77541

Received June 14, 1999; Revised Manuscript Received August 25, 1999

ABSTRACT: Ethylene−styrene interpolymers (ESIs) are viewed as random copolymers of ethylene and ethylene−styrene dyads. The amorphous ESIs offer an approach to characterizing polyethylene without the constraints imposed by the inevitable crystallinity. Large strain, nonlinear stress relaxation and recovery of ESIs were studied at temperatures above the glass-transition temperature (T_g). The nonlinear stress relaxation curves superposed on the double-logarithmic scale by vertical shifting after a characteristic time τ_k that increased as the molecular weight increased and the testing temperature approached T_g. The experimental shift factors were independent of molecular weight and styrene content and correlated well to the damping function obtained in the tube theory. The instantaneous recovery after stress relaxation increased as the molecular weight increased or as the testing temperature decreased approaching T_g. Instantaneous recovery was correlated with stress relaxation in terms of mechanisms of molecular dynamics. The success of this approach led to a generalization of the model of two coexisting networks used previously.

Introduction

Recently, interest in copolymers of ethylene and styrene has been stimulated by the development of metallocene and single-site constrained-geometry catalysts[1−3] that make it possible to synthesize copolymers with large amounts of styrene.[4] The copolymers of ethylene and styrene used in this and previous studies have substantially random incorporation of styrene except that successive head-to-tail styrene chain insertions are shown by ^{13}C NMR analysis to be absent, even with high levels of styrene incorporation.[4] For this reason, the polymers are described as "pseudorandom" ethylene−styrene interpolymers (ESIs). Because there are no styrene−styrene dyads, it is useful to consider the ESIs as random copolymers of ethylene and ethylene−styrene dyads.

A previous publication describes the systematic correlation of copolymer composition with crystallinity, density, dynamic mechanical response, and tensile deformation behavior.[5] A composition of about 50 wt % styrene marks a gradual transition from semicrystalline to amorphous polymers. The transition occurs as incorporation of the noncrystallizable styrene comonomer gradually reduces the number of crystallizable ethylene sequences. The glass-transition temperature of amorphous polymers increases with increasing styrene content from below to above ambient temperature. The amorphous polymers with glass-transition temperature below ambient temperature behave as rubberlike liquids; the elastic characteristics are attributed to the entanglement network. Amorphous polymers with glass-transition temperature slightly above ambient temperature exhibit glassy behavior at short times and rubbery behavior at longer times.

The remarkable temperature and rate sensitivity of amorphous ESIs in the ambient temperature range is a motivation for studying their viscoelastic behavior. A previous investigation of the creep behavior of amorphous ESIs in the glass-transition region demonstrated excellent time−temperature superposition.[6] The entanglement molecular weight obtained from the retardation time spectrum and the plateau compliance was found to be much closer to polyethylene than to polystyrene, probably because of the unique chain microstructure of ESIs with no styrene−styrene dyads. Thus, regarding chain flexibility and the entanglement network, ESIs provide an unusual opportunity to approach the amorphous phase of polyethylene without the constraints imposed by the inevitable crystallinity. Furthermore, because of statistical homogeneity in comonomer content over the entire molecular weight distribution, ESIs can serve as a benchmark for studying the dependence of viscoelastic behavior on copolymer composition.

The focus of this paper is to study the large strain, nonlinear stress relaxation and strain recovery behavior of amorphous ESIs at temperatures above the T_g, where the viscoelastic behavior is in the plateau and terminal regions and stress relaxation is related to the dynamics of the transient entanglement network. By use of the copolymers of different comonomer contents and molecular weights, the mechanisms of stress relaxation that are most influenced by these parameters can be explored. At present, the molecular dynamics is best described by the tube theory incorporating the concept of chain reptation.[7] Nonlinearity, i.e., dependence of stress relaxation on imposed strain, is an immediate outcome of reptation dynamics, and systematic data to test the theoretical expectations are essential. Recent studies reveal that, in accordance with the tube theory, the nonlinear relaxation modulus of most linear polymer melts can be factorized:

$$E(t, \lambda) = h(\lambda)E(t) \quad (1)$$

where $h(\lambda)$ is the damping function.[8−11] However, most

* To whom correspondence should be addressed.
[†] Case Western Reserve University.
[‡] The Dow Chemical Company.

10.1021/ma990938g CCC: $18.00
Published on Web 10/15/1999

Table 1. Materials for the Relaxation and Recovery Study

code	styrene (wt %)	a-PS (wt %)	T_g (°C)	$10^{-3} \times M_w$ (g/mol)	M_w/M_n
ES52	52	1.5	−2	219	2.4
ES62	62	2.9	12	219	2.6
ES60 (350)	61	0.7	10	349	2.3
ES60 (250)	60	0.5	8	252	2.4
ES60 (160)	58	0.5	6	164	2.5
ES60 (120)	58	0.6	4	119	2.6

of these studies used shear deformation or constant strain rate uniaxial tension rather than a direct relaxation experiment. In the present study, the relaxation is studied using uniaxial tension.

Theoretical understanding of recovery behavior lags far behind that of stress relaxation. Attempts to formulate a molecular interpretation of recovery date to the model of two coexisting networks brought forth by Tobolsky in the 1940s.[12] The utility of this concept was further demonstrated in subsequent work of Taylor and Ferry[13] and Djiauw and Gent.[14] From a discussion of this concept in connection with the relaxation data, an approach that correlates instantaneous recovery and stress relaxation in terms of mechanisms of molecular dynamics, and thereby generalizes the model, is proposed.

Experimental Section

Materials. The ESIs synthesized by INSITE technology (INSITE™ is a trademark of The Dow Chemical Company.) are described in Table 1. The composition and molecular weight data were provided by Dow. The polymers contained a very small amount of atactic styrene homopolymer (aPS). The weight percent styrene in the copolymer and the amount of aPS were obtained by NMR. The polymers are designated by the prefix ES, followed by weight percent styrene in the copolymer. The molecular weight was included in the designation of polymers used in the molecular weight study. The glass-transition temperature was measured by dynamic mechanical thermal analysis (DMTA) at a frequency of 1 Hz with a tensile strain less than 0.2%. The temperature was raised from 50 °C below T_g to 30 °C above T_g at a scanning rate of 3 °C/min. The glass-transition temperature was taken at the maximum of the loss tangent peak.

Methods. Plaques 1.3 mm thick were compression molded from pellets at 190 °C and cooled at about 15 °C/min using conditions described previously.[6] A rectangular specimen was cut from the plaque. Reference lines were drawn on the center of the specimen to obtain the draw ratio, defined as the ratio of the length after loading to the initial length.

The stress relaxation response was measured in uniaxial extension. Specimens were stretched to the desired draw ratio in an Instron machine. The sample length and the stretching speed were varied to obtain a stretching time at about 1 s. The maximum speed used was 500 mm/min. The deformation was recorded with a video camera with a telescopic lens attachment to obtain the draw ratio. The stress was recorded continuously beginning approximately 5 s after stretching in order to avoid initial instabilities. After the specimen relaxed for some period of time, the lower grip was released. The time required to physically separate the lower grip was less than 0.2 s. Therefore, recovery measurements were started 1 s after grip release, and the recovery at 1 s after was defined as the instantaneous recovery.

All the experiments were carried out in an environmental chamber. The temperature variation during an experiment was less than 0.2 °C, and the temperature gradient inside the chamber was also less than 0.2 °C. To study the effect of composition, ES52 and ES62 were used and experiments were performed at 23 °C. In the molecular weight studies, all of the measurements were carried out 15 °C above T_g.

Results and Discussion

Nonlinear Stress Relaxation Behavior. The stress relaxation curves of ES52 at different applied strains are shown in Figure 1. The modulus $E(t,\lambda)$ was defined by the following equation:

$$E(t,\lambda) = 3\sigma(t)/(\lambda^2 - \lambda^{-1}) \quad (2)$$

where $\sigma(t)$ is the true tensile stress and λ is the applied draw ratio during relaxation. If the draw ratio was 1.1 or less, $E(t,\lambda)$ was independent of the applied strain and the polymers exhibited linear stress relaxation behavior. However, if the draw ratio was 1.3 or larger, the ESIs exhibited nonlinear stress relaxation behavior. It may be concluded that the strain limit for linear viscoelastic behavior is between 10 and 30% for the ESIs. A similar strain limit was reported for polystyrene and styrene−butadiene melts.[9,15]

For a molecular interpretation of nonlinear relaxation, it is useful to consider the concepts of the Doi−Edwards tube theory.[7] In this theory, each chain is confined in a tube that is bent at the entanglement points and is straight between them. The tube forms a primitive path for the chain. Upon imposition of strain, the chain deforms affinely and the primitive path contour length increases. After an instantaneous deformation, the stress relaxes in the three steps shown in Figure 2. In step 1, "Rouse-like" short-range relaxation lowers the stress to the rubbery plateau value. This occurs through local rearrangement of the chain segments within the fixed entanglements. This step finishes within time τ_e, which depends on the number of monomer units between entanglements but not on the molecular weight. For $t < \tau_e$, there is no influence of applied strain on the modulus, and the material exhibits linear behavior. In step 2, which occurs at times $t > \tau_e$, the entire chain retracts inside the stretched tube in order to restore the contour length of the original primitive path. In this step, the chain segments redistribute themselves by slipping through the entanglements. Because the difference between the contour lengths of the original and the deformed tubes depends on the imposed strain, stress relaxation is nonlinear. As this step finishes, the chain is completely relaxed within the tube but preserves its nonequilibrium orientation. The last step (step 3) has been called disengagement because the chain diffuses out of the original tube by reptation motions. Having diffused out, the chains are randomly oriented. The residual stress is proportional to the fraction of chains that remains confined in the deformed tube, which decreases with time. The characteristic times of steps 2 and 3, τ_R and τ_d, depend on molecular weight as M^2 and M^3, respectively. Step 3 accounts for relaxation in the terminal region.

The Doi−Edwards theory predicts that in step 3 the relaxation modulus can be factorized by the product of the damping function $h(\lambda)$ and the linear relaxation modulus $E(t)$. In the rigorous treatment, the damping function is derived as

$$h(\lambda) = \frac{15}{8}\frac{\lambda(2\lambda^3+1)}{(\lambda^3-1)^2}\frac{1}{1+A(\lambda)}\left[1 - \frac{4\lambda^3-1}{2\lambda^3+1}A(\lambda)\right] \quad (3)$$

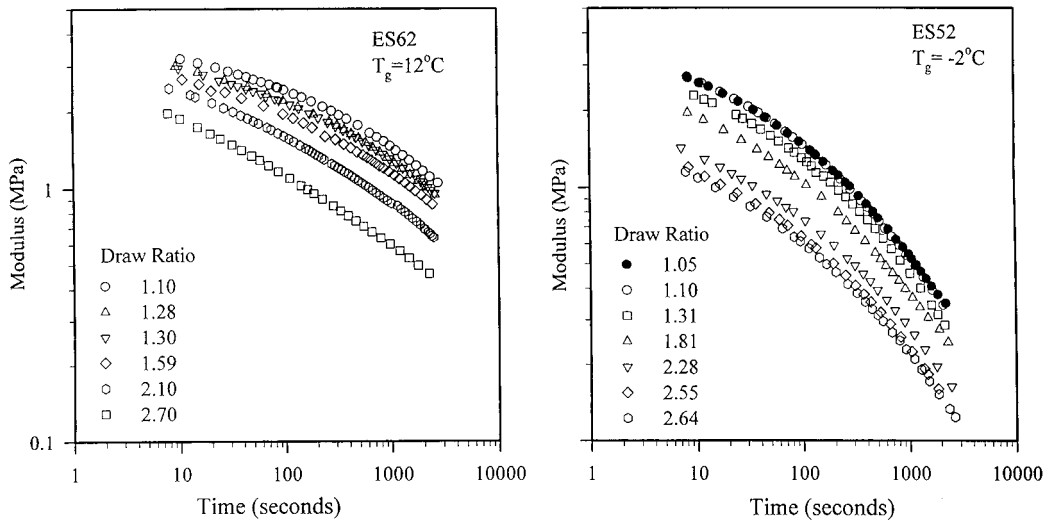

Figure 1. Effect of applied strain on stress relaxation of ES62 and ES52 at 23 °C.

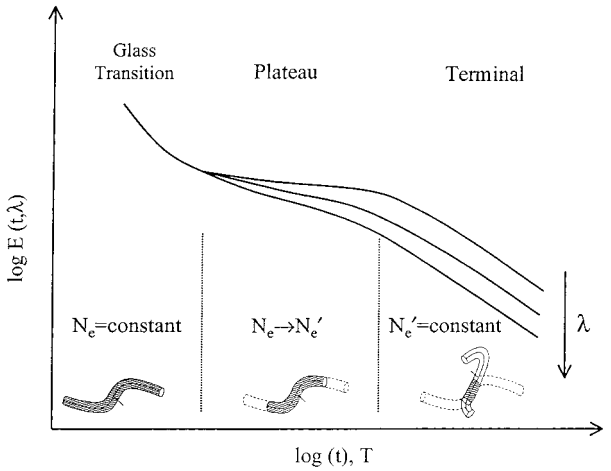

Figure 2. Schematic of the effects of different relaxation mechanisms in the Doi−Edwards theory on the time or temperature dependence of the relaxation modulus E at different strains λ.

where

$$A(\lambda) = \frac{\sinh^{-1}\sqrt{\lambda^3 - 1}}{\sqrt{\lambda^3(\lambda^3 - 1)}} \tag{4}$$

In a simplified form of the theory, each strand of the primitive path is assumed to deform independently (independent alignment assumption). In this case, $h(\lambda)$ can be written as

$$h(\lambda) = \frac{5}{\lambda^2 - \lambda^{-1}}\left[\frac{3}{2}\frac{\lambda^3}{\lambda^3 - 1}\left(1 - \frac{\tan^{-1}\sqrt{\lambda^3 - 1}}{\sqrt{\lambda^3 - 1}}\right) - \frac{1}{2}\right] \tag{5}$$

Equation 1 suggests that the curves $E(t,\lambda)$ at different strains can be superimposed by vertical shifting on a double-logarithmic plot of modulus versus time. The reduced relaxation curves, $E(t,\lambda)/h(\lambda)$, were obtained by shifting the nonlinear stress relaxation curves toward the linear stress relaxation curve. The results for ES52 and ES62 at 23 °C are plotted in Figure 3. The relaxation curves of ES62 superposed only at long times. The time where superposition started was defined as τ_k. For ES62, τ_k was about 500 s. However, for ES52, the relaxation curves superposed in their entirety; hence, τ_k was shorter than the loading time. Because the glass-transition temperature of ES52 was well below the testing temperature, the first and second relaxation steps finished too rapidly to appear in the experimental time scale, and only the third relaxation step was observed. In contrast, the relaxation curve of ES62 included contributions of step 2 that were responsible for nonsuperposition at short times.

The reduced relaxation curves for ES60s of different molecular weights are plotted in Figure 4. Superposition started at longer times as the molecular weight increased. The value of τ_k is a measure of the time when the relaxation step 2 completes and should be on the same order of magnitude as the characteristic time τ_R of step 2, which is the longest Rouse relaxation time in the absence of the topological restraints. Indeed, it is reported that the ratio τ_k/τ_R is between 4 and 5 for most linear polymer solutions and melts.[10,16,17] It is further observed that both τ_k and τ_R are proportional to the square of the molecular weight for melts and solutions of polymers with sharp molecular weight distributions.[16,17] Because the ESIs under investigation are not monodisperse, there should exist a distribution for τ_k and τ_R. This results in a smoother transition from steps 2 to 3 and difficulties in picking τ_k for ESIs. Nevertheless, it is apparent that τ_k increased with increasing molecular weight.

The experimental values of the damping function $h(\lambda)$ that gave the reduced relaxation curves are plotted in Figure 5. The values were independent of styrene content and molecular weight. This is consistent with eqs 3 and 5, which do not include any molecular parameters (e.g., molecular weight and chemical structure). The calculated damping functions from eqs 3 and 5 are also shown in Figure 5. The damping functions were derived rigorously and, with the independent alignment assumption, were very similar for uniaxial tension. Both described the experimental results well.

Although good agreement between the experimental damping function and the Doi−Edwards model is generally observed for linear polymers under shear deformation,[10,18] there is some controversy when the polymer is under uniaxial deformation: some researchers report that the model underestimates the damping function.[18−20] Conversely, others find fairly good agreement for polystyrene with a narrow molecular weight distribution.[9] However, most of the damping functions

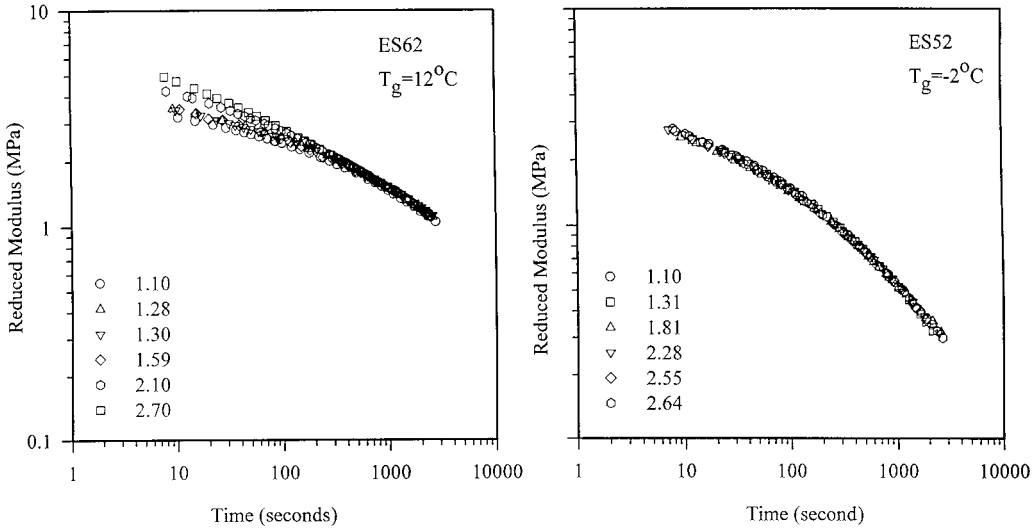

Figure 3. Reduced stress relaxation curves of ES62 and ES52 at 23 °C.

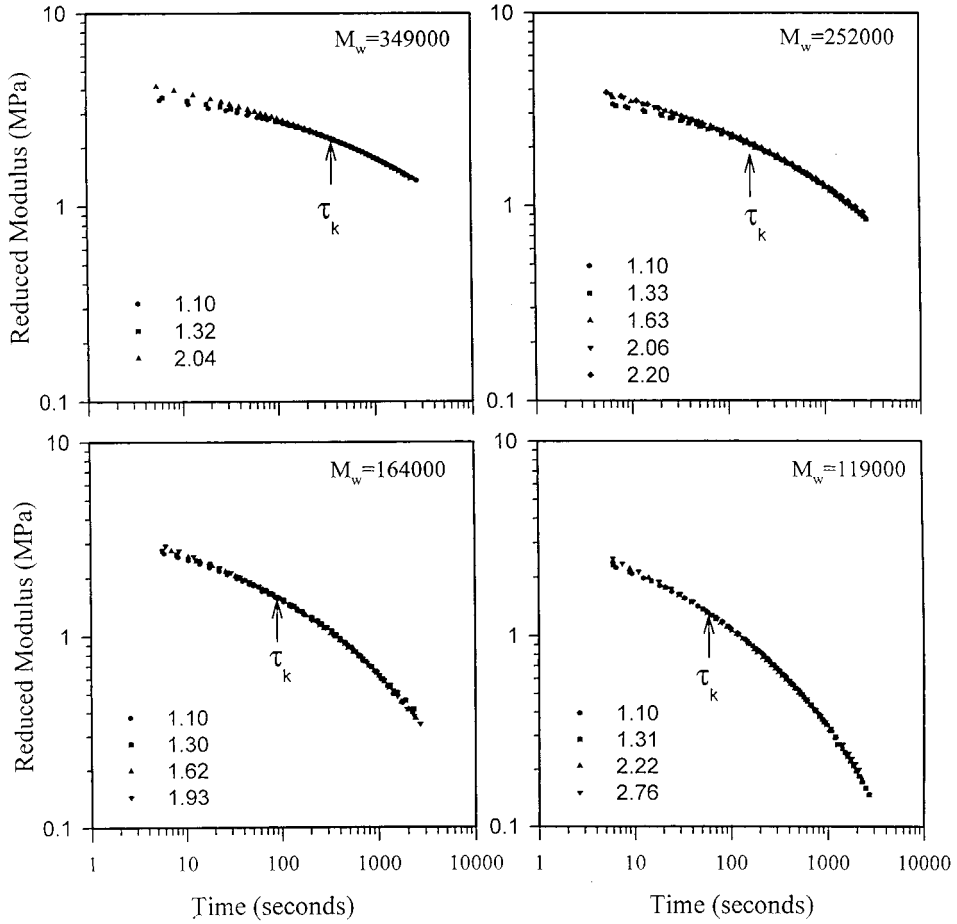

Figure 4. Effect of molecular weight on the reduced relaxation curves of ES60 at T_g + 15 °C.

in uniaxial tension were obtained from a constant rate extension experiment rather than from stress relaxation.

Instantaneous Recovery after Stress Relaxation. The instantaneous unrecovered strain after stress relaxation was defined as

$$S_r = (\lambda_r - 1)/(\lambda_o - 1) \quad (6)$$

where λ_r is the draw ratio at 1 s after unloading and λ_o is the imposed draw ratio during relaxation. The results are tabulated in Tables 2−4. For all of the materials tested, the instantaneous recovery decreased as the relaxation time increased. At 23 °C, the instantaneous recovery was less for ES52, which was further above the glass-transition temperature, than that for ES63. In addition, the instantaneous recovery decreased with decreasing molecular weight.

In one of the few attempts to analyze recovery of linear polymers after stress relaxation in the plateau and terminal regions, Djiauw and Gent (DG) describe recovery in terms of a two-network model.[14] During

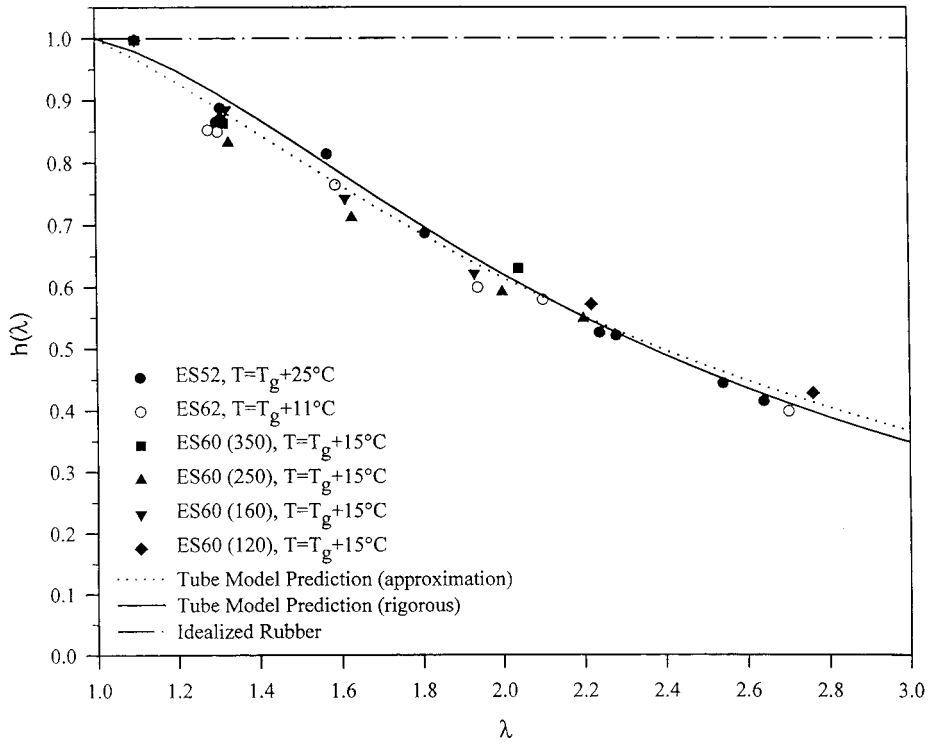

Figure 5. Comparison of the damping function from stress relaxation with the tube model prediction.

Table 2. Instantaneous Unrecovered Strain for ES62 at 11 °C above T_g

relax. time (min)	draw ratio (λ_o)	remaining stress (frac.) (f_o)	S_i (%) (obsd)	S_i (%) (DG model)
40	1.28	0.26	68	69
	1.60	0.22	68	68
	2.20	0.18	68	66
0.5	2.20	0.62	23	23
2	2.04	0.51	34	33
10	2.10	0.34	50	48
40	2.20	0.18	68	66

Table 3. Instantaneous Unrecovered Strain for Materials with Different Molecular Weight at 15 °C above T_g

	relax. time (min)	draw ratio (λ_o)	remain. stress (frac.) (f_o)	S_i (%) (obsd)	S_i (%) (DG model)
ES60 (350)	0.5	2.00	0.68	20	20
T_g + 15°C	2	2.03	0.54	29	30
	10	1.97	0.40	44	43
	40	1.98	0.27	60	57
ES60 (250)	0.5	2.20	0.65	22	21
T_g + 15°C	2	2.04	0.51	36	33
	10	2.11	0.33	52	48
	40	2.09	0.21	68	63
ES60 (160)	0.5	2.05	0.63	25	24
T_g + 15°C	2	2.02	0.40	49	43
	10	2.08	0.22	70	61
	40	1.95	0.10	82	80

relaxation, the original ("old") entanglement network is partially replaced by a "new" entanglement network, whose strands are in their equilibrium conformations. The transient stress is proportional to the fraction of remaining entanglements because the new entanglement network is not load-bearing. The total number of entanglements is assumed to be constant. After the stress is relieved, the new entanglement network is in compression and the old network is in tension. Furthermore, the strain states of new and old networks are different. For the old network, the draw ratio is λ_r because its equilibrium state is the unstretched state

Table 4. Instantaneous Unrecovered Strain for ES52at 25 °C above T_g

relax. time (min)	draw ratio (λ_o)	remain. stress (frac.) (f_o)	S_i (%) (obsd)	S_i (%) (DG model)	S_i (%) (modified model)
2	1.27	0.36	61	58	59
	1.77	0.36	56	50	57
	2.30	0.36	55	43	57
40	1.30	0.07	89	91	92
	1.60	0.07	91	89	91
	2.20	0.07	90	84	90
0.5	2.31	0.53	39	29	42
2	2.32	0.36	55	43	58
10	2.25	0.18	77	64	76
40	2.20	0.07	90	84	90

before relaxation. The compression ratio for the new network is λ_r/λ_0 because the equilibrium state for the new network is the stretched state during relaxation. Assuming that both networks behave as classical rubber networks, the stress on the old network σ_0 is equal to $E_0F_e(\lambda_r^2 - 1/\lambda_r)$, and the stress on the new network σ_n is equal to $E_0(1 - F_e)[(\lambda_r/\lambda_o)^2 - \lambda_o/\lambda_r)$, where F_e is the fraction of remaining old entanglements and E_0 is the original network modulus. The value of F_e is taken as the ratio f_0 of the stress after relaxation to the initial stress. By assuming that the true stresses in both networks are equal after releasing the load,

$$f_0(\lambda_r^2 - 1/\lambda_r) + (1 - f_0)(\lambda_r^2/\lambda_0^2 - \lambda_0/\lambda_r) = 0 \qquad (7)$$

the draw ratio λ_r at instantaneous recovery can be obtained. Thus, the instantaneous unrecovered strain, S_r in eq 6, can be predicted from the relaxation experiment. Because some stress relaxation occurs during the loading and unloading time, it is usual to take the initial stress and the instantaneous recovery at the same delay time after loading or unloading.[13,14] It is assumed thereby that these uncontrollable changes in the networks roughly compensate each other. The initial stress

at 1 s was obtained by extrapolating the relaxation curve from 5 s.

The instantaneous recovery predicted by the DG model is compared with the experimental results in Tables 2−4. For ES62 at 23 °C (12 °C above the T_g), the instantaneous recovery is well-described by this model for all values of initial strain and relaxation time (Table 2). The stress relaxation of this material had pronounced nonlinearity; nevertheless, the model fit very well. For the ES60 series materials, which had slightly lower glass-transition temperatures, the model described recovery for the material with the highest molecular weight quite well (Table 3). However, with decreasing molecular weight, the model started to deviate, especially for longer relaxation times. The deviation was most noticeable for ES52, the material with the lowest T_g, at the larger strains (Table 4). Systematic deviation from the DG model with the molecular structure suggested a deeper look at the assumptions of the model.

Although the two-network model is built on a simplistic intuitive basis, the model, in general, resulted in good predictions of instantaneous recovery. However, the original structural interpretation of relaxation in terms of entanglement replacement is not entirely consistent with the Doi−Edwards tube theory. In particular, the assumption that the number of entanglements remains constant during relaxation cannot hold. By definition, the number of entanglements changes during relaxation step 2, chain retraction.[7] This has been confirmed in experiments that combine simultaneous measurements of dynamic moduli with large strain stress relaxation.[21,22] Furthermore, characterizing the elastic response of both relaxed and deformed networks by the same modulus, that of the original network E_0, is not well-justified. This was realized previously: Taylor and Ferry attempted to generalize the DG model by expressing the modulus of the old network in the Mooney−Rivlin nonlinear form with coefficients dependent on the relaxation time but assuming linear behavior of the new network.[13,23] However, any description based on Mooney−Rivlin coefficients has the well-known disadvantage that no molecular or structural interpretation is possible.

Good correlation between the model and experiment probably stems from the fundamental validity of the two-network concept, with the recognition that resistance of the relaxed part of the network is a major factor opposing recovery upon release of the stress. However, rather than appealing to entanglement concepts, the origin of the two networks can be better understood in terms of relaxation dynamics of different chain units. In a real material, there exists a broad distribution in the parameters describing the rate of relaxation on scales of both a chain and a subchain between entanglements. First, molecular weight distribution dramatically affects the chain retraction and disengagement time scales. Second, variations in the subchain contour length between entanglements, as well as variations in the length and in the orientation of the primitive path segment, affect subchain relaxation rate. The relaxation stress in the Doi−Edwards theory was calculated by averaging over these variations. In addition, there is a distribution in the "ease of slip" of the subchain through an entanglement; this was not taken into account in the original relaxation theory[7] but was realized later in the tube theory of elasticity.[24] The last factor is particularly important for short chain branched copolymers because of the inherent nonuniformity in branch placement along the chain. These differences result in populations of subchains that relax on different time scales. After the initial deformation, all populations contribute to the decreasing residual stress by relaxing, and the averaged description is appropriate. However, upon release of the load, populations on the edges of the distribution act in opposite ways. By the rough grouping of the populations as long- and short-term relaxing populations, the former, bearing the residual stress, drive recovery, and the latter, having already reached an equilibrium configuration, resist recovery.

This interpretation of the two networks leads to reformulation of the DG model in terms of the amount of material in the relaxed and stressed populations. The questionable assumption of conservation in the number of entanglements is replaced by a requirement that the total amount of material in all populations of subchains be constant, which is obviously valid. To arrive at eq 7, it is only necessary to assume that, first, the elastic response is rubberlike and, second, the specific moduli of both networks are the same.

The first assumption is inherent to the concept of instantaneous recovery. The second assumption needs further discussion. Comparison of the quality of the DG fit, Tables 2−4, with the relaxation behavior, Figures 3 and 4, suggests a justification for the second assumption on the basis of structural arguments. The instantaneous unrecovered strain obtained from eq 7 excellently fit the recovery data for materials whose relaxation did not involve step 3, chain disengagement. Chain diffusion out of the initial tube did not occur on the experimental time scale because of either proximity to the glass-transition temperature, as for ES62, or high molecular weight, as for ES60(350). The nonlinear relaxation curves of these materials did not superpose except for a small region at longer times. The major relaxation mechanism was identified as step 2, chain retraction. Whether chains or their parts had retracted more or less to their equilibrium lengths determined whether they belonged to the new or the old network populations. However, independently of this, the chains remained confined in the affinely deformed, original tube structure. It is reasonable to ascribe the same specific modulus to both networks in this case. This modulus may be affected by the imposed strain, but similarly for all subchain populations because they all belong to the same (original) tube system and the damping function does not depend on molecular weight. Equation 7 applies except that F_e is redefined as the fraction of the subchain population in the old unrelaxed network. As before, F_e is taken as equal to the ratio of the stress after relaxation to the initial stress.

The instantaneous unrecovered strain obtained from the DG model did not fit the recovery data for materials whose relaxation involved step 3, chain disengagement. This can be seen for ES52 (Figure 3 and Table 4) and for the ES60 series at longer relaxation times and lower molecular weights (Figure 4 and Table 3). The assumption that the old, unrelaxed and the new, relaxed subchain populations have the same modulus is no longer valid if step 3 contributes significantly to relaxation. If relaxation occurred by disengagement over the entire time scale of relaxation, as was the case for ES52, the tube structure of the new network would entirely be reconstructed. This network would be built from

completely relaxed, randomly oriented chains and therefore would be identical to the original network. The elastic response of the new network would be characterized by the modulus of the original network (the rubber plateau modulus) and is taken to be the linear modulus of the original network at 1 s. Linear relaxation does not include chain retraction, step 2, and therefore the damping function is unity. In contrast, the old network at large imposed strain passed through step 2 relaxation during the 1 s loading time. This decreased its modulus by the damping function $h(\lambda_0)$ because of the partial adaptation of the chain conformations to the deformed tube confinement. Again assuming a rubberlike response upon instantaneous recovery, the balance of stresses between the two networks is written as

$$h(\lambda_0)f_0(\lambda_r^2 - 1/\lambda_r) + (1 - f_0)(\lambda_r^2/\lambda_0^2 - \lambda_0/\lambda_r) = 0 \quad (8)$$

which determines λ_r, and subsequently, the instantaneous irrecoverable strain S_r is obtained from eq 6. Equation 8 differs from eq 7 in the appearance of the damping function. It provides a modification of the DG model for the case of relaxation by the chain disengagement. Table 4 shows excellent correlation between the observed instantaneous recovery strain for ES52 and that predicted from eq 8.

In summary, statistically homogeneous ethylene−styrene interpolymers provided a good model system for examining the molecular dynamics of stress relaxation and recovery. By strongly affecting both stress relaxation and recovery, changing comonomer content revealed the different mechanisms of molecular relaxation for chemically similar materials on the laboratory time scale at temperatures close to ambient. At large imposed strains, relaxation of ESIs showed pronounced nonlinearity that was amenable to interpretation in terms of tube theory. Experimental values of the damping function obtained by superposition of nonlinear relaxation curves fit the theory well. Furthermore, although comonomer content and molecular weight influenced the relaxation dynamics, neither affected the damping function, again consistent with theoretical predictions. An analysis of recovery that considered the tube theory mechanisms of relaxation led to a new interpretation of the two-network model and extended the time/temperature range over which this model is an effective predictive tool for instantaneous recovery.

Acknowledgment. The authors thank Drs. Martin J. Guest and Y. Wilson Cheung of The Dow Chemical Company for providing technical assistance. The financial support of The Dow Chemical Company is gratefully acknowledged.

References and Notes

(1) Miyatake, T.; Mizunuma, K.; Kakugo, M. *Makromol. Chem., Macromol. Symp.* **1993**, *66*, 203−214.
(2) Ren, J.; Hatfield, F. R. *Macromolecules* **1995**, *28*, 2588−2589.
(3) Xu, G.; Lin, S. *Macromolecules* **1997**, *30*, 685−693.
(4) The Dow Chemical Company. U.S. Patent 5,703,187; E.P. Patent 416,815A1.
(5) Chen, H.; Guest, M. J.; Chum, S.; Hiltner, A.; Baer, E. *J. Appl. Polym. Sci.* **1998**, *70*, 109−119.
(6) Chen, H. Y.; Stepanov, E. V.; Chum, S.; Hiltner, A.; Baer, E. *J. Polym. Sci., Part B: Polym. Phys.* **1999**, *37*, 2373−2382.
(7) Doi, M.; Edwards, S. F. *The Theory of Polymer Dynamics*; Oxford University Press: Oxford, U.K. 1986; p 118.
(8) Osaki, K. *Rheol. Acta* **1993**, *32*, 429−437.
(9) Urakawa, O.; Takahashi, M.; Masuda, T.; Ebrahimi, N. G. *Macromolecule*s **1995**, *28*, 7196−7201.
(10) Takahashi, M.; Isaki, T.; Takigawa, T.; Masuda, T. *J. Rheol.* **1993**, *37*, 827−846.
(11) Larson, R. G. *J. Rheol.* **1985**, *29*, 823−831.
(12) Andrews, R. D.; Tobolsky, A. V.; Hanson, E. E. *J. Appl. Phys.* **1946**, *17*, 352−361.
(13) Taylor, C. R.; Ferry, J. D. *J. Rheol.* **1979**, *23*, 533−542.
(14) Djiauw, L. K.; Gent, A. N. *J. Polym. Sci., Symp.* **1974**, *48*, 159−165.
(15) Merriman, H. G.; Caruthers, J. M. *J. Polym Sci., Polym. Phys. Ed.* **1981**, *19*, 1055−1071.
(16) Osaki, K.; Nishimura, Y.; Kurata, M. *Macromolecules* **1985**, *18*, 1153−1157.
(17) Osaki, K.; Takatori, E.; Tsunashima, Y.; Kurata, M. *Macromolecules* **1987**, *20*, 525−529.
(18) Mead, D. W.; Larson, R. G.; Doi, M. *Macromolecules* **1998**, *31*, 7895−7914.
(19) Wagner, M. H.; Ehrecke, P. *J. Rheol.* **1998**, *42*, 621−638.
(20) Wagner, M. H. *Rheol. Acta* **1990**, *29*, 594−603.
(21) Isono, Y.; Itoh, K.; Komiyatani, T.; Fujimoto, T. *Macromolecules* **1991**, *24*, 4429−4432.
(22) Isono, Y.; Nishitake, T. *Polymer* **1995**, *36*, 1635−1638.
(23) Noordermeer, J. W. M.; Ferry, J. D. *J. Polymer. Sci., Polym. Phys. Ed.* **1976**, *14*, 509−520.
(24) Edwards, S. F.; Viglis, T. A. *Rep. Prog. Phys.* **1988**, *51*, 243−297.

MA990938G